# Tissue motion in blood velocity estimation and its simulation

**Schlaikjer, Malene; Torp-Pedersen, Søren; Jensen, Jørgen Arendt; Stetson, Paul F.**

*Published in:*
IEEE Ultrasonics Symposium Proceeding

*Link to article, DOI:*
10.1109/ULTSYM.1998.765228

*Publication date:*
1998

*Document Version*
Publisher's PDF, also known as Version of record

# Tissue motion in blood velocity estimation and its simulation

M. Schlaikjer[1], S.T. Petersen[2], J.A. Jensen[1], P.F. Stetson[1]

[1]Department of Information Technology, Build. 344,
Technical University of Denmark, DK-2800 Lyngby, Denmark
[2]Department of Radiology, Gentofte University Hospital,
Niels Andersensvej 65, DK-2900 Hellerup, Denmark

## Abstract

Determination of blood velocities for color flow mapping systems involves both stationary echo canceling and velocity estimation. Often the stationary echo canceling filter is the limiting factor in color flow mapping and the optimization and further development of this filter is crucial to the improvement of color flow imaging. Optimization based on *in-vivo* data is difficult since the blood and tissue signals cannot be accurately distinguished and the correct extend of the vessel under investigation is often unknown. This study introduces a model for the simulation of blood velocity data in which tissue motion is included.

Tissue motion from breathing, heart beat, and vessel pulsation were determined based on *in-vivo* RF-data obtained from 10 healthy volunteers. The measurements were taken at the carotid artery at one condition and in the liver at three conditions. Each measurement was repeated 10 times to cover the whole cardiac cycle and a total of 400 independent RF measurements of 950 pulse echo lines were recorded. The motion of the tissue surrounding the hepatic vein from superficial breathing had a peak velocity of 6.2±3.4 mm/s over the cardiac cycle, when averaged over the 10 volunteers. The motion due to the heart, when the volunteer was asked to hold his breath, gave a peak velocity of 4.2±1.7 mm/s. The movement of the carotid artery wall due to changing blood pressure had a peak velocity of 8.9±3.7 mm/s over the cardiac cycle. The variations are due to differences in heart rhythm, breathing, and anatomy. All three of these motions are handled independently by the simulation program, which also includes a parametric model for the pulsatile velocity in the elastic vessel. The model can be used for optimizing both color flow mapping and spectral display systems.

## 1 Introduction

Estimates of blood velocity in human vessels can be obtained from recorded ultrasound RF signals. These signals consist of components from both blood and surrounding tissue, and separation of the signals is needed to visualize only the blood velocities. This filtration is crucial to the estimation process, and the optimization of this necessitates well-defined data. *In-vivo* RF-data is not usable, since the blood and the tissue signals cannot be accurately distinguished and the correct extend of the vessel under investigation is often unknown. Instead simulated data that incorporates all relevant features of the measurement situation could be employed. One feature is the motion in the tissue surrounding the vessels induced by breathing, heartbeat, and pulsation of arterial vessel walls. Pulsation arises from the pumping action of the heart, which forces a pulsating blood flow into the arteries, thereby creating a time varying pressure which acts on the vessel wall [1]. The motion in the tissue is a result of a change in position of one or more organs (lung and heart) and vessel walls lying close to the region of interest (ROI). The motion changes the position of the ROI and can also change the size of the different components in the region (e.g. increased diameter of vessel because of pulsation). The motion repeats it self due to the periodic nature of breathing and heartbeat. The repetition time and thereby duration of the motion are usually not the same for the individual motion contributors. On average the heartbeat frequency is about 60 beats/min, and the respiratory frequency 12 breaths/min (when resting), but varies among individuals and their physical state.

The level of motion will vary between scan sites depending on the distance from inducer to ROI and the motion level of the inducer (e.g. breathing level: superficial or deep). The question is whether the motion can be detected, and whether it influences the velocity estimation. If this is the case, realistic models of the individual motion contributors have to be developed and incorporated into a realistic simulation program of the signals. This study investigates the presence of motion and suggests motion models - developed from investigation of *in-vivo* data. The models are then used in a simulation of RF ultrasound data in which both the spatially varying and pulsatile blood flow are modeled together with tissue motion from both vessel pulsation, breathing, and heart movement.

0-7803-4095-7/98/$10.00 

The simulation is based on the Field II program [2, 3] using spatial impulse response and point scatterers. Using this program any array transducer, focusing, apodization, and transducer excitation can be handled.

## 2 System and recording conditions

To develop models for the individual motion contributors, a number of measurements at different positions and under various conditions were performed. Table 1 lists the scan sites and the motions present during measurements. The carotid artery and hepatic vein were chosen, since these sites reveal information about the different motions. In addition it is possible to introduce conditions, so that the recordings only contain information about one or more of the motions at the time. Pulsation is only present in arteries but some pulsation - although very small - is also seen in veins. Therefore pulsation is also included as a possible motion for the hepatic vein. In the HV1 recordings the hepatic vein would have moved outside the ROI, if the volunteers were allowed to breath normally. Therefore they were directed to breath only superficially to allow part of the hepatic vein to remain within the ROI. To eliminate influence from breathing in HV2, the volunteers were asked to hold their breath while measuring.

| Dataset | Vessel | Scan plane | Motion |
|---|---|---|---|
| C1 | Carotid artery | Transverse scan angle $90^o$ | P,B |
| HV1 | Hepatic vein | Right liver lobe intercostal scan | B,H (P) |
| HV2 | Hepatic vein | Right liver lobe intercostal scan | H (P) |
| HV3 | Hepatic vein | Left liver lobe epigastric scan | H (P) |

Table 1: Recording conditions for determination of motion due to pulsation (P), heart (H) and breathing (B).

The measurements were performed with a 3.2 MHz probe on a B&K 3535 ultrasound scanner connected to a dedicated, real-time sampling system [4] capable of acquiring 0.27 seconds of data for one RF-line. The probe was hand-held during measurements. Measurements were performed on 10 healthy volunteers lying in the supine position. Each measurement was repeated 10 times to cover the whole cardiac cycle and a total of 400 independent RF measurements of 950 pulse echo lines were recorded. It was not possible to synchronize the measurements to the ECG signal, and it could therefore not be guaranteed that the whole heart cycle was covered in the complete measurement set for each volunteer.

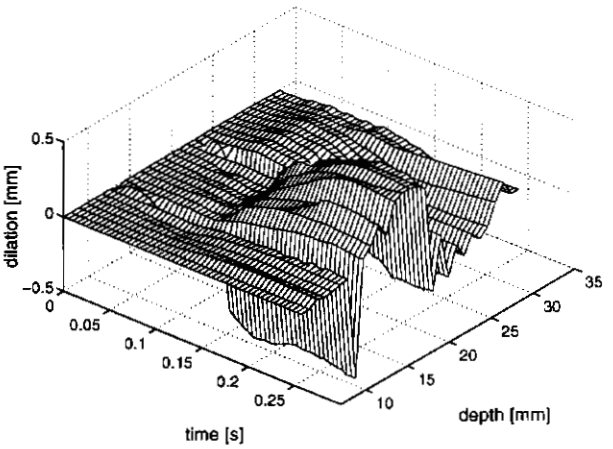


Figure 1: Example of dilation found from *in-vivo* data from the carotid artery. Pulse rate: 70 bpm.

## 3 Models developed from *in-vivo* data

The RF-data were bandpass filtered and the tissue velocities estimated by applying the autocorrelation method [5]. Thirty-four adjacent RF-lines were used to obtain high-quality estimates. Tissue velocity estimates as a function of time and depth were thereby determined for further investigation. The estimates revealed presence of motion in the tissue. The maximum velocity ($v_{max}$) estimates averaged over the 10 volunteers and standard deviation ($\sigma_v$) among these are listed in Table 2.

| | C1 | HV1 | HV2 | HV3 |
|---|---|---|---|---|
| $v_{max}$ | 8.9 mm/s | 6.2 mm/s | 4.2 mm/s | 10.1mm/s |
| $\sigma_v$ | 3.7 mm/s | 3.4 mm/s | 1.7 mm/s | 3.0 mm/s |

Table 2: Maximum velocities and corresponding standard deviations obtained for the 4 scan conditions.

The velocities in the tissue are small compared to the usual velocity levels seen in the center of an artery, that are in the order of 3-4 m/s. The blood velocities are however lower and goes to zero at the vessel wall. The blood and tissue velocities thereby have similar levels at the boundary. Distinguishing the signals belonging to blood and tissue is therefore complicated. The maximum velocities quantify the level of motion as well as the influence from the different motion contributors and the dependence on distance. By comparing the obtained maximum velocities from each volunteer for the different scan sites using a Wilcoxon test, knowledge of these features can be obtained. Comparing HV1 and HV2 gives a $p$-value of 0.01, revealing that the heart influences the motion at the right liver lobe, and the presence of respiration adds to the motion. Whether there is a dependence on distance can be

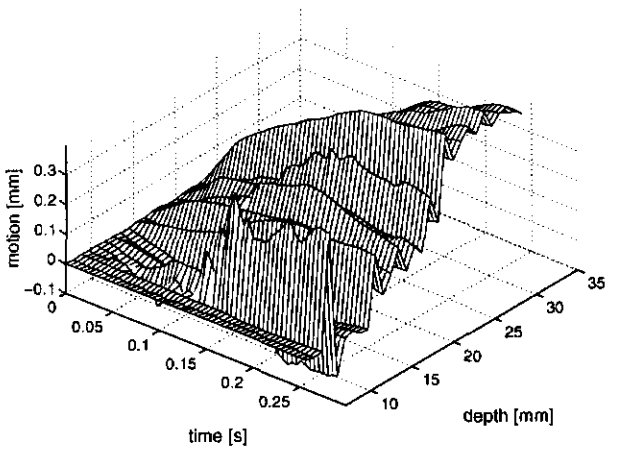


Figure 2: Example of breathing motion at carotid artery.

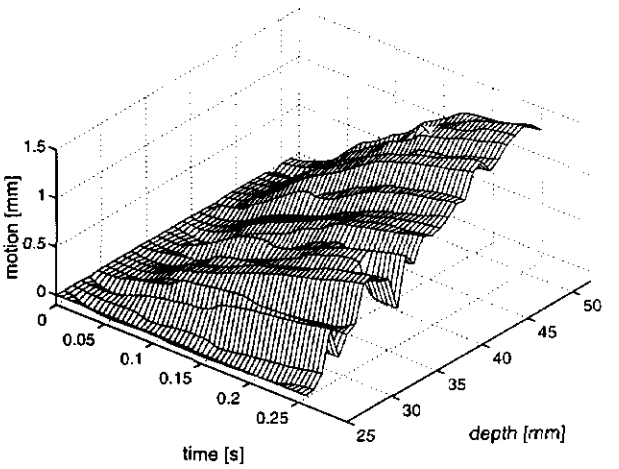


Figure 3: Example of motion due to heartbeat (HV3) at hepatic vein.

revealed by testing HV2 against HV3. The $p$-value for this is 0.004, so there is a significant difference in motion between the two scan sites.

Based on this investigation it can be concluded that tissue motion is present, and should be incorporated into the simulation program to obtain realistic simulated data.

The development of a simulation model was based on plots of velocity and dilation or motion estimates as a function of time and depth. Dilation and motion is obtained by a time integration of the estimated velocities at each depth:

$$d(n\Delta T) = \sum_{i=0}^{n} v(i\Delta T, z)\Delta T \qquad (1)$$

where $n$ is the estimate number, $\Delta$T the time between estimates, $v(..)$ the estimated velocities, and $z$ the depth. Figures 1, 2 and 3 show examples of dilation plots, which visualizes features of the 3 different motions over time and depth. The dilation is positive if the scatterers move towards the transducer relative to an initial position, and negative if movement is away from the transducer.

## 3.1 Pulsation

In Fig. 1 dilation estimates from the carotid artery are visualized. The motion present is due to pulsation, since motions in opposite directions are seen. The onset of the pulsation occurs at the time equal to 0.12 seconds. Dilation estimates before that gives information about the dilation sequence, when returning to the initial position from the previous pulsation. This part also reveals two opposite motions - with decreasing amplitude. The nature of pulsation [1] shows, that the position change of tissue scatterers has to be controlled by a change in radius relative to the center of the vessel. The time sequence of the dilation rises fast and then decreases and returns to the initial value. The motion is damped radially. Less dilation is seen with increased radius relative to the center. The model therefore is a function of time and depth, and assuming that there is no correlation between time and depth, the motion model becomes a product of two functions - one describing the time sequence, and the other describing the depth dependence. The damping function can be a linear or exponential dependence as a function of radius. In Fig. 4(a) the model for pulsation for a given depth is shown with a choice of pulse rate of 1 pulse/s. This model matches the *in-vivo* dilation estimates obtained by Bonnefous [6].

## 3.2 Breathing

An example of motion due to breathing during inhalation is seen in Fig. 2. The lung is positioned deeper than the scanned region, explaining why the tissue is moving towards the transducer, and the level of motion increases as a function of depth. The exact motion direction of the lung wall is unknown, so the motion is modeled as acting along the axial axis - corresponding to what is seen in the motion plot. Motion due to breathing is a much slower process than pulsation due to the respiration frequency. Breathing can be modeled as a product of a damping and time dependent function, when it is assumed that they are independent. The time sequence at a given depth is shown in Fig. 4(b). The model has a negative sign, since the motion is acting in the opposite direction of the positive axial axis ($z$-axis).

## 3.3 Heartbeat

A sequence of motion due to the heart beating is shown in Fig. 3. It contains the same features as for breathing regarding

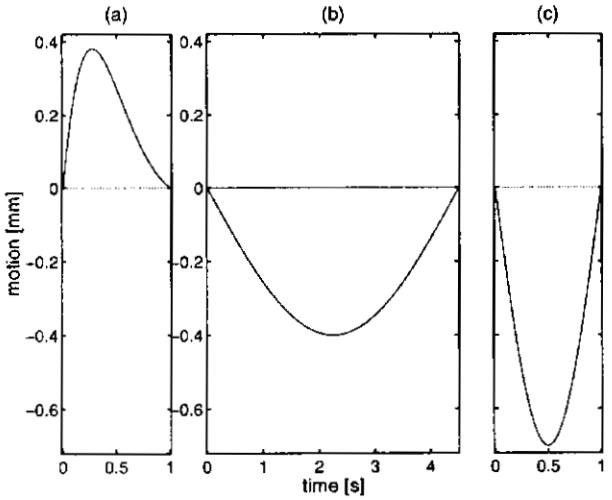


Figure 4: Models of dilation due to pulsation (a), breathing (b) and heartbeat (c). Frequency of breath: 13 breaths/min, pulsation and heartbeat: 60 pulses/min.

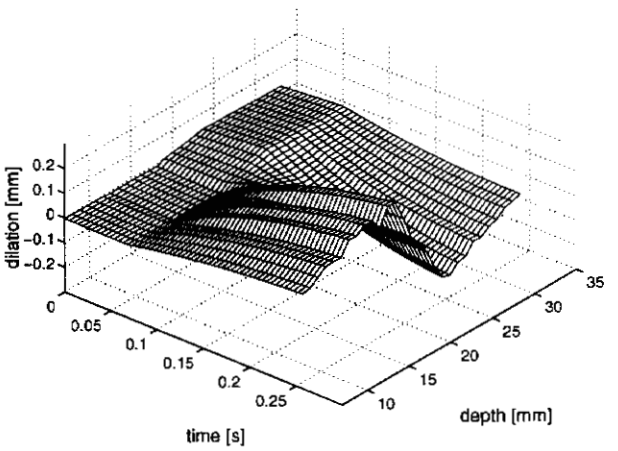


Figure 5: Estimates of dilation from simulated data mainly due to pulsation at the carotid artery. Pulse rate: 60 bpm.

position of motion generator, damping, and time sequence, but the repetition frequency is lower - in average 1 beat/s. A model for the heartbeat motion is given in Fig. 4(c), again assuming that the motion is acting in the axial direction.

All the models developed contain the same features regarding time and depth dependence, but the repetition time, amplitude of motion, and damping vary with scan site and for the individual motion types. Additionally these model parameters vary among individuals. Assuming no correlation between the individual motions, the accumulated tissue motion at a given scan site can be calculated by adding the individual motion vectors.

# 4 Simulations of motion

The transducer was modeled as a 3.2 MHz convex, elevation focused array with 58 elements. A focusing and apodization scheme matching the used scan probe was incorporated. The point scatterers were given amplitude properties of tissue or blood, and moved around according to the the motion model between each simulation of an RF-line. The motion of the blood scatterers was determined by Womersley's pulsatile flow model [7, 8]. RF-data equal to 5 seconds were simulated, thereby having data containing the full effect of pulsation, heartbeat and breathing. In Fig. 5 an example of simulated dilation for the carotid artery is shown, when pulsation and breathing motion was incorporated. The damping was modeled by a linear function, and the scan angle was $90^o$.

The breathing motion is at this point in the simulation not very dominant. Comparing with Fig. 1 reveals a good agree-

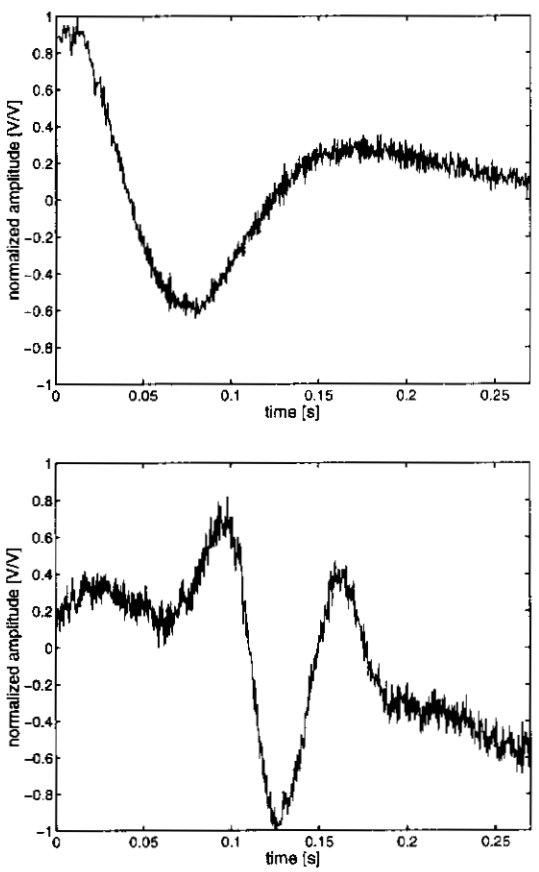


Figure 6: A measured and simulated RF-line at the vessel wall as a function of time.

ment between the two dilations. Notice that the pulse rates differ for the two plots, giving a faster pulsation sequence for the high pulse rate. Perfect match to this one example of real dilation is obtainable by adjusting amplitude and possible by introducing an exponential damping function. These are variables that vary relative to scan site, respiration and pulsation level, and patient, and these can be set in the simulation model. In the plot of *in-vivo* dilation also some motion is present within the vessel (center of vessel at depth equal to 19 mm) - probably because the scan angle was not exactly $90^o$.

In Fig. 6 a comparison of real and simulated RF-data at the vessel wall of the carotid artery as a function of time is shown. The tissue motion is seen as the slow varying signal component, and on top of that is the blood signal. Again the simulated and real data agree qualitatively.

# 5 Conclusion

Based on the above investigation it can be concluded that tissue motion is present, and should be incorporated in a simulation program to create realistic simulated data. It is possible to model tissue motion and incorporate this into a simulation program. The simulated RF-data agree well with *in-vivo* RF-data, making the simulation a realistic and powerful tool in optimizing ultrasound echo canceling filters and blood velocity estimators.

# 6 Acknowledgement

This project is supported by grant 9700883 and 9700563 from the Danish Science Foundation, grant 980018-311 from the Technical University of Denmark, and by B-K Medical A/S, Denmark.

# References

[1] W.W. Nichols and M.F. O'Rourke. *McDonald's Blood Flow in Arteries, theoretical, experimental and clinical principles*, Lea & Febiger, 1990.

[2] J.A. Jensen and N.B. Svendsen. *Calculation of pressure fields from arbitrarily shaped, apodized, and excited ultrasound transducers*, IEEE Trans. Ultrason., Ferroelec., Freq. Contr., 39, pp. 262-267, 1992.

[3] J.A. Jensen. *Users' guide for the Field II program*, Technical report, Dept. of Info. Tech., Techn. Univ Denmark, 1998.

[4] J.L. Jensen and J. Mathorne. *Sampling system for in-vivo ultrasound images*, Medical Imaging V Symposium, SPIE vol. 1444, pp. 221-231, 1991.

[5] C. Kasai, K. Namekawa, A. Koyano and R. Omoto. *Real-time two-dimensional blood flow imaging using an autocorrelation technique*, IEEE Trans. Son. Ultrason., 32:458-463, 1985.

[6] O.Bonnefous. *Stenoses dynamics with Ultrasonic Wall Motion Images.* In Proc. 1994 IEEE Ultrasonics Symposium, pp. 1709-1712, 1994.

[7] J.R. Womersley. *Oscillatory motion of a viscous liquid in a thin-walled elastic tube. I: The linear approximation for long waves.* Phil. Mag., 46:199-221, 1955.

[8] D.H. Evans. *Some aspects of the relationship between instantaneous volumetric blood flow and continuous wave Doppler ultrasound recordings III.* Ultrasound Med. Biol., 9:617:623, 1982b.

[9] J.A. Jensen. *Estimation of Blood Velocities Using Ultrasound, A signal processing approach*, Cambridge University Press, 1996.